

《Technical Report》

**Radiation Shielding Calculation on Shield System of CANDU 6
Plant Using the Coupled DOT4.2 and QAD-CG Codes**

Kyo Youn Kim

Korea Atomic Energy Research Institute

Jong Kyung Kim

Hanyang University

(Received July 5, 1993)

**DOT4.2-QAD-CG 접속법을 이용한 CANDU 6 발전소
차폐 계통에 대한 방사선 차폐 계산**

김교윤

한국원자력연구소

김종경

한양대학교

(1993. 7. 5 접수)

Abstract

DOT4.2-QAD-CG coupling method was used to analyze the dose rates outside the side and the bottom shield system of CANDU 6 plant. The average dose rates at the main airlock and the new fuel loading area are approximately $6 \mu\text{Sv/h}$ as it is required. The calculated dose rates have a good agreement with the measurements at the operating CANDU 6 plant. The method used in this paper can be applied to the radiation shielding analysis of Wolsong 2, 3, and 4 CANDU 6 type plants which will be constructed in the near future.

요 약

CANDU 6 발전소의 측면 및 하단 차폐 구조에서의 방사선 선량율을 해석하기 위하여 DOT4.2-QAD-CG 접속 방법을 이용한 평가 방법이 시도되었다. 평가 결과에 의하면 주 출입구 및 신연료 장전 구역에서의 평균 방사선 선량율은 설계 목표치인 약 $6 \mu\text{Sv/h}$ 정도로 나타났으며, 또한 이러한 평가 결과는 CANDU 6 발전소에서의 실험치와도 잘 일치하고 있음을 확인할 수 있었다. 따라서, 본 논문에서 사용된 평가법은 앞으로 건설 될 CANDU 6 원자로인 월성 2, 3 및 4호기의 방사선 차폐해석에도 이용될 수 있을 것이다.

1. Introduction

It is very important to confirm that the dose rate level at the accessible areas in nuclear power plant is as low as accessible during reactor operation. However, it is not easy and not simple to calculate the dose rates at these areas since it is complicate to model the reactor building system geometrically and to process the source term to be considered in computer code calculations. In the past, the dose rates outside the concrete vault wall of CANDU 6 reactor were obtained by using the analytical methods, a one dimensional removal diffusion code MAC-RAD⁽¹⁾, and a one dimensional discrete ordinates transport code ANISN⁽²⁾. However it is not easy to calculate the dose rate at some desired points besides mesh mid-point, and there are some factors to be considered to correct the finite length of calandria and non-uniformity of its source strength. In this study DOT4.2⁽³⁾-QAD-CG⁽⁴⁾ coupling method is thus considered to analyze the dose rates at the accessible areas of the CANDU 6 power plant. DOT4.2-QAD-CG coupling method and its applications to CANDU 6 reactor are introduced at following sections. The calculational results using DOT4.2-QAD-CG coupling method are compared with the measured values at the operating CANDU 6 reactor.

2. DOT4.2-QAD-CG Coupling Method

The radiation shielding analysis on outside the side and the bottom shield system of CANDU 6 reactor was performed by using a two-dimensional discrete ordinates transport code DOT4.2 and a point kernel integration code QAD-CG.

DOT4.2 code is used to calculate the volume-integrated thermal neutron fluxes and the thermal neutron flux distributions in mainshell, annular plate, and subshell of the calandria during reactor operation. Mainshell, annular plate, and subshell

of the calandria are used as the source regions of QAD-CD model. The volume-integrated thermal neutron fluxes are used as total source strengths in the source region of QAD-CG model. The axial and the radial thermal neutron flux distributions are used as the axial and the radial neutron capture gamma source distributions, respectively, in the source regions of QAD-CG model. Those data from DOT4.2 results are then incorporated into a QAD-CG analysis for the calculation of gamma dose rates outside the side and the bottom shield system during reactor operation.

Since the multi-source region is not available in QAD-CG code, 12 QAD-CG calculations have to be performed for each dose point. In other word, main shell, annular plate, and subshell as the source region are sectionalized to 4 regions ($z = -Z \sim 0$ and $z = 0 \sim Z$ for $\phi = 0 \sim \pi$ and $\phi = \pi \sim 2\pi$, respectively, for $r = R_i \sim R_o$), respectively. The contributions from 12 source regions were summed to calculate total dose rate at each dose point.

3. Application to CANDU 6 Reactor

A two-dimensional discrete ordinates transport code DOT4.2 was used in R-Z geometry to calculate the thermal neutron flux distributions in main-shell, annular plate, and subshell of the calandria under the condition of reactor operation.

A 38 energy-group scheme derived from DLC-37⁽⁵⁾, which is composed of 27 neutron and 11 gamma energy groups, was used for this calculation. The 27 neutron energy groups include 7 fast neutron groups ($E_n \geq 0.82$ MeV), 19 intermediate neutron groups (0.414 eV $\leq E_n < 0.82$ MeV), and 1 thermal neutron group ($E_n < 0.414$ eV).

The radial and the axial fission density distributions were calculated from the time-average bundle power distributions⁽⁶⁾ as shown in Tables 1 and 2, respectively.

GIP code, which is a part of DOT4.2, was used

to prepare a group cross-section library. The microscopic cross-sections from the library have been mixed, in the same run, to obtain the macroscopic cross-sections for the materials.

In this study a P_3 order of scattering and a S_6 order of angular quadratures were used⁽⁷⁾. The geometrical set up for the DOT4.2 calculation is shown in Figure 1. A 59 axial and 65 radial mesh structure for the 28 regions was used.

A few iterative DOT4.2 runs were made to reach the desired flux convergence level for the thermal neutron group and other groups. The criterion used in the calculations is 0.002. The thermal neutron flux distributions are obtained in the calandria main shell, annular plate, and sub-shell and those are given in Tables 3, 4, and 5, respectively.

The dose rates outside the concrete vault walls are mostly due to the neutron capture gammas in the calandria during reactor operation. In other word, operating core gammas including fission

product decay gammas do not contribute to the dose rates outside the concrete vault walls. Thus, the core gammas were not considered in this work.

Table 1. Radial Fission Density Distribution on Vertical Mid-Plane of Reactor Used in DOT4.2

Radial Distance from Core Center (cm)	Fission Density [fission/cm ³ .s]
257.2	5.45E+11
260.3	5.35E+11
266.7	5.14E+11
273.0	4.91E+11
279.4	4.67E+11
285.7	4.43E+11
292.1	4.17E+11
298.4	3.90E+11
304.8	3.60E+11
311.1	3.26E+11
314.3	3.09E+11

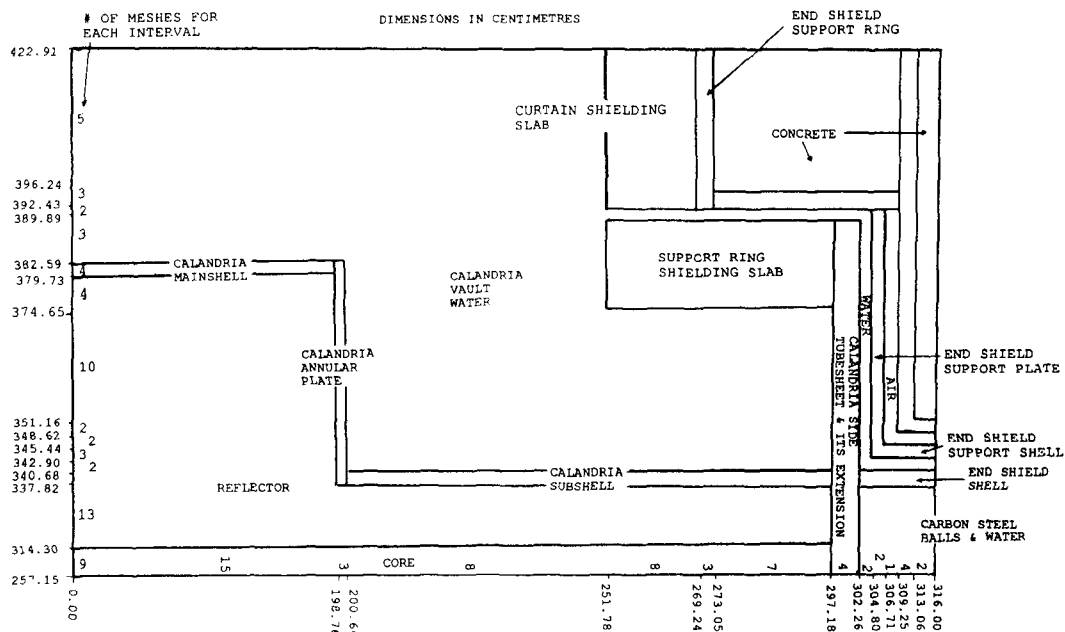


Fig. 1. Mesh Structure Used in DOT4.2 for Neutron Capture Gamma Source Calculation.

Table 2. Axial Fission Density Distribution at R = 257.17 cm Used in DOT4.2

Axial Distance from Vertical Mid-Plane (cm)	Normalized Fission Density
0.0	1.00E+00*
6.6	1.00E+00
20.6	1.00E+00
33.1	9.96E-01
46.4	9.86E-01
59.6	9.70E-01
72.6	9.49E-01
86.1	9.21E-01
99.4	8.88E-01
112.6	8.49E-01
125.9	8.04E-01
139.1	7.53E-01
152.4	6.96E-01
165.6	6.34E-01
178.9	5.69E-01
192.1	4.98E-01
199.1	4.60E-01
199.7	4.57E-01
200.3	4.54E-01
204.3	4.32E-01
211.6	3.94E-01
218.9	3.55E-01
226.2	3.18E-01
233.5	2.82E-01
240.8	2.47E-01
248.1	2.15E-01
255.4	1.84E-01
259.6	1.67E-01
260.7	1.63E-01
261.8	1.59E-01
262.9	1.55E-01
264.0	1.51E-01
265.1	1.47E-01
266.2	1.43E-01
267.1	1.39E-01
268.0	1.36E-01
268.8	1.34E-01
271.6	1.24E-01
176.2	1.10E-01
280.9	9.62E-02
285.5	8.41E-02
290.2	7.33E-02
294.9	6.41E-02
297.2	6.00E-02

* Corresponds to 5.45×10^{11} fission/cm³.s

The thermal neutron capture gamma source spectrum in unit of γ/s per cm in steel per unit flux is given in Table 6, which was taken from TAPEMAKER, a part of ANISN code, run of Kim's calculations⁽⁸⁾. It should be noted that the sources for the group 28 and the groups 36~38 were not considered in the analysis because they are too small in magnitude of source strength and very low in source energy, respectively.

The volume-integrated thermal neutron fluxes in main shell, annular plate, and subshell of the calandria, i.e., 4.835×10^{18} n.cm/s, 8.872×10^{17} n.cm/s, and 1.654×10^{18} n.cm/s, respectively, are calculated from DOT4.2 calculations. The distributions (both axial and radial) of the thermal neutron flux in the calandria obtained from the DOT4.2 calculations were used for gamma source distribution in QAD-CG code.

Figures 2 and 3 show the dose points in QAD-CG model to calculate the dose rates for the areas outside the primary side and the bottom shield during reactor operation. The dose points are located at the outer surface of the reactor wall concrete, the new fuel loading area, the stairway in the main lobby area, and the main airlock area as shown in Figure 2. Figure 3 also shows 8 specific dose points on contact with the bottom shield.

It is noted that the calculated dose rates were all due to gammas in the energy range 10.0~7.0 MeV. As given in Table 6, all gammas in this energy range were treated as 8.5 MeV gammas which have the highest yield in the source spectrum. In fact, many gammas have energies lower energies than this energy. It is thus necessary to correct for the true gamma spectrum by using the gamma yields. Lone et al.⁽⁹⁾ calculated the gamma yields for iron, chromium, nickel, and manganese, which are basic constituents of steel, as a function of gamma energy. These yields (cross-section weighted) are grouped in four energy groups and the corresponding gamma yields are given in Table 7. This shows that the dominant gamma

Table 3. Thermal Neutron Flux Distribution in the Calandria Main Shell

Radial Distance from Core Center (cm)	Thermal Neutron Flux (n/cm ² .s)	Axial Distance from Core Center (cm)	Thermal Neutron Flux ^e (n/cm ² .s)
379.73 ^a	1.05E+13	0.00 ^c	1.05E+13
380.09	9.03E+12	6.63	9.03E+12
380.80	4.83E+12	19.89	8.95E+12
381.52	2.91E+12	33.13	8.95E+12
382.23	2.04E+12	46.38	8.70E+12
382.59 ^b	1.70E+12	59.63	8.69E+12
		72.88	8.26E+12
		86.13	8.19E+12
		99.38	7.61E+12
		112.63	7.41E+12
		125.88	6.65E+12
		139.13	6.23E+12
		152.38	5.21E+12
		165.63	4.32E+12
		178.88	2.85E+12
		192.14	1.36E+12
		198.76 ^d	9.42E+11

- a. Main Shell Inner Radius = 379.73 cm
b. Main Shell Outer Surface = 382.59 cm
c. Main Shell Center Line = 0.0 cm
d. Main Shell End = 198.76 cm
e. Flux at the Reflector Wall

energy is approximately 7.7 MeV and not 8.5 MeV. The revised dose rates, based on 0.0549 γ /s and 0.147 yields for 6.0 MeV and 8.5 MeV gammas, respectively, were calculated by using the gamma release rates given in Table 7. Then the correction factor, 0.487, was obtained from the ratio of this revised dose rate to the QAD-CG dose rate for total energy group. The actual dose rates at 24 dose points were thus obtained from multiplying this correction factor to QAD-CG dose rates.

Flux-to-dose rate conversion factors used in QAD-CG calculations were taken from radiological health handbook⁽¹⁰⁾.

4. Results and Discussion

The actual dose rates are given in Table 8. The dose rates outside the side shield (accessible areas during reactor operation) are given at 16 specific dose points as shown in Figure 2. The dose rates on contact with the bottom shield are given at 8 specific dose points (ceiling of the room that contains the fuelling machine auxiliaries) as shown in Figure 3. The average dose rates at the main airlock and the new fuel loading area are approximately 6 μ Sv/h as a design target. Although the dose rates at other points are higher than 6 μ Sv/h, it is still acceptable since occupancy of

Table 4. Thermal Neutron Flux Distribution in the Annular Plate

Radial Distance from Core Center (cm)	Thermal Neutron Flux (n/cm ² .s)	Axial Distance from Core Center (cm)	Thermal Neutron Flux ^e (n/cm ² .s)
337.82 ^a	3.02E+13	198.76 ^c	3.02E+13
338.26	2.77E+13	199.08	2.77E+13
339.14	2.26E+13	199.71	2.12E+13
340.02	2.04E+13	200.34	1.77E+13
340.57	1.96E+13	200.66 ^d	1.76E+13
341.05	1.88E+13		
341.79	1.79E+13		
342.53	1.70E+13		
343.32	1.60E+13		
344.17	1.53E+13		
345.01	1.37E+13		
347.35	1.02E+13		
349.67	1.07E+13		
350.52	1.08E+13		
351.37	9.77E+12		
353.69	6.80E+12		
357.48	5.35E+12		
361.28	4.34E+12		
365.07	3.40E+12		
368.87	2.61E+12		
372.66	1.90E+12		
375.42	1.72E+12		
377.15	1.34E+12		
378.87	9.33E+11		
380.09	6.15E+11		
380.80	3.71E+11		
381.52	2.39E+11		
382.23	1.69E+11		
382.59 ^b	1.48E+11		

a. Annular Plate Inner Radius = 337.82 cm

b. Annular Plate Outer Radius = 382.59 cm

c. Annular Plate Inner Surface = 198.76 cm

d. Annular Plate Outer Surface = 200.66 cm

e. Flux at the Reflector Wall

these areas will be low during reactor operation.

The calculated dose rates were also compared with the dose rates from the measurements at Point Lepreau power plant⁽¹¹⁾, CANDU 6 reactor being operated over the eight years. The measured dose rates are given in Table 8. For the

cases considered, it appears that the calculated dose rates outside the side and the bottom shield agree well within approximately 20% uncertainty at the specific dose points except for the new fuel loading area with the measured values documented in Reference 11.

Table 5. Thermal Neutron Flux Distribution in the Subshell

Radial Distance from Core Center (cm)	Thermal Neutron Flux (n/cm ² .s)	Axial Distance from Core Center (cm)	Thermal Neutron Flux ^e (n/cm ² .s)
337.82 ^a	1.55E+13	200.66 ^c	1.55E+13
338.26	1.28E+13	204.31	1.28E+13
339.14	6.39E+12	211.61	9.26E+12
340.02	4.29E+12	218.92	7.79E+12
340.57	3.73E+12	226.22	6.66E+12
340.68 ^b	3.80E+12	233.52	5.81E+12
		240.82	5.07E+12
		248.13	4.42E+12
		255.43	3.85E+12
		259.62	3.57E+12
		260.71	3.46E+12
		261.80	3.34E+12
		262.89	3.26E+12
		263.98	3.15E+12
		265.07	3.06E+12
		266.16	2.97E+12
		267.12	2.88E+12
		267.87	2.80E+12
		268.82	2.72E+12
		271.57	2.50E+12
		276.23	2.13E+12
		280.28	1.76E+12
		285.54	1.38E+12
		290.20	9.85E+11
		294.85	5.46E+11
		297.18 ^d	2.76E+11

a. Subshell Inner Radius = 337.82 cm

b. Subshell Outer Radius = 340.68 cm

c. Subshell Inner Surface = 200.66 cm

d. Subshell Outer Surface = 297.18 cm

e. Flux at the Reflector Wall

5. Conclusion

It is concluded that the calculated dose rates using DOT4.2-QAD-CG coupling method have a good agreement with the measurements at the operating CANDU 6 power plant. The method applied in this work can be used for radiation shielding analysis of Wolsong 2, 3, and 4 CANDU plants which will be constructed in Korea in the

near future.

References

1. U. Canali, H. Ilsemann, C. Ponti, and H. Preusch, "MAC-RAD, A Reactor Shielding Code," European Atomic Energy Community-EURATOM, EUR 2152.e (1964)
2. W.W. Engle, Jr., "A Users Manual for AISN-A

Table 6. Thermal Neutron Capture Gamma Source Spectrum for Steel

DOT4.2 Group No. (Gammas)	Energy Range (MeV)	E_γ^a (MeV)	Σ_{ic}^b ($\gamma/s.cm$ per unit flux)
28	14.00-10.00	12.00	4.66E-7
29	10.00-7.00	8.50	1.47E-1
30	7.00-5.00	6.00	5.49E-2
31	5.00-3.00	4.00	5.17E-2
32	3.00-2.00	2.50	3.67E-2
33	2.00-1.50	1.75	3.01E-2
34	1.50-1.00	1.250	1.46E-2
35	1.00-0.40	0.70	4.28E-2
36	0.40-0.20	0.30	2.39E-2
37	0.20- 0.10	0.15	5.80E-3
38	0.10-0.01	0.055	6.44E-2

a. Mean Energy for Each Group

b. Thermal Neutron Capture Gamma Source Spectrum for Gamma Group i

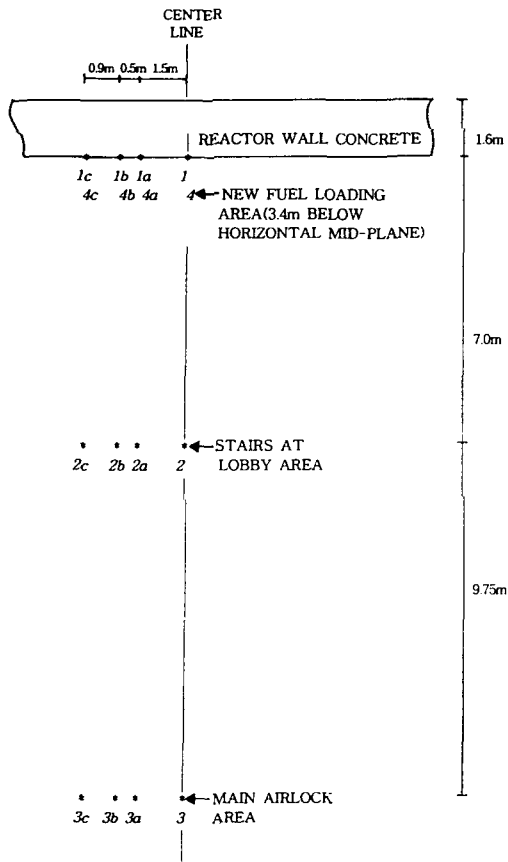


Fig. 2. QAD-CG Dose Points Outside Reactor Wall Concrete (Plane View)

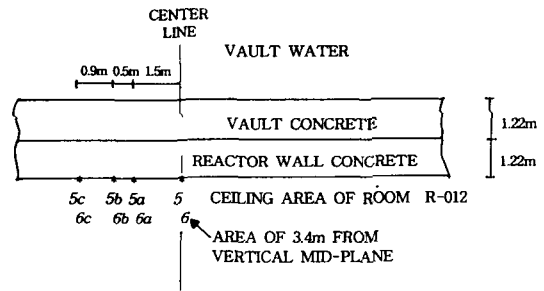


Fig. 3. QAD-CG Dose Points Outside Reactor Wall Concrete (Section View)

Table 7. Neutron Capture Gamma Release Rates in Steel Calculated from Data Given in Reference 6

Energy Range	Average Energy ^a (MeV)	Gamma Yield (γ /disintegration, %)
6.84-7.27	7.07	5.5
7.27-7.94	7.65	39.6
7.94-8.53	8.48	4.9
8.53-9.72	9.08	15.0

a. Average Energy for Gamma Decay %.

Table 8. Comparison of the Calculated Dose Rate with the Measured Dose Rate

Dose Point	Calculated Dose Rate ($\mu\text{Sv/h}$)	Measured Dose Rate ^a ($\mu\text{Sv/h}$)
1	70.0	
1a	46.0	
1b	33.0	10.0–75.0
1c	15.0	
2	21.0	
2a	18.0	
2b	16.0	10.0–25.0
2c	13.0	
3	6.9	
3a	6.0	
3b	6.0	6.0
3c	5.6	
4	6.4	
4a	3.7	
4b	2.9	Less than 10.0
4c	1.5	
5	49.0	
5a	34.0	
5b	25.0	10.0–40.0
5c	12.0	
6	5.6	
6a	3.9	
6b	3.0	Less than 10.0
6c	1.5	

a. Reference 11

One-Dimensional Discrete Ordinates Transport Code with Anisotropic Scattering”, K-693, Union Carbide Corporation (1967)

3. W.A. Rhoades, “DOT IV Version 4.2-Two-Dimensional Discrete Ordinates Radiation Transport Code System,” RSIC Computer Code Collection, CCC-320, Oak Ridge National Laboratory, Oak Ridge, Tennessee (1979)
4. V.R. Cain, “QAD-CG-A Combinatorial Geometry Version of QAD-P5A, A Point Kernel Integration Code for Neutron and Gamma Ray Shielding Calculations,” RSIC Computer Code Collection, CCC-307, Oak Ridge National Laboratory, Oak Ridge, Tennessee (1979)
5. W.E. Ford, “Coupled 100 Neutron-21 Gamma Ray Group, P₈ Cross Section Library for EPR,” ORNL/TM-5249, Oak Ridge National Laboratory, Oak Ridge, Tennessee (1976)
6. A.L. Wight and R. Sibley, “Fuel Management Design Program-FMDP,” AECL Report TDAI-105, Atomic Energy of Canada Limited, Mississauga, Ontario (1977)
7. J.P. Jenal, “The Generation of A Computer Library for Discrete Ordinates Quadrature Sets,” ORNL/TM-6023, Oak Ridge National Laboratory, Oak Ridge, Tennessee (1977)
8. K.Y. Kim and J.K. Kim, “Nuclear Energy Depositions in the Primary End Shields and Side Primary Shield Systems,” J. of Korean Association for Radiation Protection, **17**, 37 (1992)
9. M.A. Lone, R.A. Leavitt, and D.A. Harrison, “Catalogue of Prompt Gamma Ray from Thermal-Neutron Capture,” Atomic Data and Nuclear Data Tables **26**, 511 (1981)
10. J.C. Villforth and M.G.R. Shultz, “Radiological Health Handbook,” U.S. Department of Health, Education, and Welfare (1970)
11. Point Lepreau Generating Station, Quarterly Technical Reports, PLGS-QTR-4-83 to -90.